remote sensing

MDPI

Article

The Use of Vis-NIR-SWIR Spectroscopy and X-ray Fluorescence in the Development of Predictive Models: A Step forward in the Quantification of Nitrogen, Total Organic Carbon and Humic Fractions in Ferralsols

Bruna Coelho de Lima [1,*], José A. M. Demattê [2], Carlos H. dos Santos [1], Carlos S. Tiritan [1], Raul R. Poppiel [2], Marcos R. Nanni [3], Renan Falcioni [3], Caio A. de Oliveira [3], Nicole G. Vedana [3], Guilherme Zimmermann [3] and Amanda S. Reis [3]

[1] Department of Soil, Campus II, University of Oeste Paulista, Presidente Prudente 19067-175, SP, Brazil; chenrique@unoeste.br (C.H.d.S.); tiritan@unoeste.br (C.S.T.)
[2] Department of Soil Science, "Luiz de Queiroz" College of Agriculture, University of São Paulo, Piracicaba 13416-900, SP, Brazil; jamdemat@usp.br (J.A.M.D.); raulpoppiel@gmail.com (R.R.P.)
[3] Department of Agronomy, State University of Maringá, Maringá 87020-900, PR, Brazil; mrnanni@uem.br (M.R.N.); rfalcioni2@uem.br (R.F.); pg55482@uem.br (C.A.d.O.); pg405864@uem.br (N.G.V.); ra117802@uem.br (G.Z.); asreis@uem.br (A.S.R.)
* Correspondence: brunacoelho94@outlook.com.br

Abstract: The objective was to verify the performance of spectral techniques as well as validation models in the prediction of nitrogen, total organic carbon, and humic fractions under different cultivation conditions. Chemical analyses for the determination of nitrate, total nitrogen, total organic carbon, and the chemical fractionation of soil organic matter were performed, as well as spectral analyses by Vis-NIR-SWIR and X-ray fluorescence. The results of the spectroscopy were processed using RStudio v. 4.1.3, and PLSR and support vector machine learning algorithms were applied to validate the models. The Vis-NIR-SWIR and XRF spectroscopic techniques showed high performance and are indicated for the prediction of nitrogen, total organic carbon, and humic fractions in Ferralsols of medium sandy texture. However, it is important to highlight that each technique has its own characteristic mechanism of action: Vis-NIR-SWIR detects the element based on harmonic tones, while XRF is based on the atomic number of the element or elemental association. The PLSR and SVM models showed excellent validation results, allowing them to fit the experimental data, emphasizing that they are different statistical methods.

Keywords: intercropping systems; machine learning; predictions on sandy soil; ammonium; nitrate; organic matter; PLSR; SVM

Citation: Lima, B.C.d.; Demattê, J.A.M.; Santos, C.H.d.; Tiritan, C.S.; Poppiel, R.R.; Nanni, M.R.; Falcioni, R.; Oliveira, C.A.d.; Vedana, N.G.; Zimmermann, G.; et al. The Use of Vis-NIR-SWIR Spectroscopy and X-ray Fluorescence in the Development of Predictive Models: A Step forward in the Quantification of Nitrogen, Total Organic Carbon and Humic Fractions in Ferralsols. *Remote Sens.* **2024**, *16*, 3009. https://doi.org/10.3390/rs16163009

Academic Editors: Asim Biswas, Bifeng Hu, Wenjun Ji and Yongsheng Hong

Received: 22 June 2024
Revised: 9 August 2024
Accepted: 13 August 2024
Published: 16 August 2024

1. Introduction

The use of conservation agriculture systems, such as no-till or intercropping, is one way to ensure the sustainability of intensive soil management [1]. In tropical and subtropical regions, soils show a high degree of weathering, as in the case of Ferralsols or Latosols according to the US soil classification system [2,3]. In these soils, the presence of organic matter is essential, since organic matter plays a fundamental role in soil properties like cation exchange capacity, nutrient availability storage, aggregate stability, and high water retention [4].

Intercropping, or mixed cropping, is an agricultural practice that consists of the simultaneous cultivation of two or more crops in the same area with the aim of efficiently matching crop needs with available resources [5]. This system benefits soil fertility through biological nitrogen fixation when used with vegetables and increases soil conservation

through increased coverage and use of space [6]. Another pertinent point is that intercropping allows nitrogen (N) and carbon (C) to cycle in the system, increasing total organic carbon (TOC) and organic N available in the soil [7].

The tropical grasses that are commonly used in this system are *Urochloa* spp. and *Megathyrsus* spp., as they have a high potential for the production of dry matter per unit area [5]. Several cultivars of *Megathyrsus maximus* exist in Brazil, including Mombasa [8]. The Mombasa cultivar belongs to a group of fodder plants that are considered demanding for fertile soils [9]. Therefore, fertilization is extremely important for the good development of this cultivar, highlighting the high nitrogen demand and the importance of appropriate N application in intercropping systems [10].

Nitrogen is the essential element in the composition of plant cells and an essential part of the life activity of the plant. It is considered to be the most important nutrient for the development and growth of crop plants [11]. In intercropping systems, the inclusion of legumes such as Guandu beans (*Cajanus cajan*) and Java (*Macrotyloma axillare*) can contribute to the increase in C in the soil and improve N efficiency by reducing nitrate loss due to leaching [12]. In addition, intercropping with legumes can reduce the amount of nitrogen fertilizer applied, which helps to reduce the environmental damage caused by the inadequate dosage of the nutrient [12].

In contrast, in addition to the implementation of conservation management practices that reduce fertilizer use and losses, the intensification of technology for rapid quantification and determination of nutrients in soil has become a fundamental tool for promoting sustainability in soil fertility. Normally, the amount of fertilizer applied to the soil is determined based on the results of soil analysis [13]. These analyses tend to be expensive, destructive, and require the use of various chemical reagents that, if improperly disposed of, can exacerbate environmental damage. Thus, proximal remote sensing technologies make it possible to obtain information on soil properties in a practical, fast, and non-destructive way without adding chemicals, which has associated them with green soil tools [14].

The X-ray fluorescence (XRF) and Vis-NIR-SWIR spectroscopic techniques are promising tools for the determination of soil attributes. Both techniques allow soil assessment with minimal preparation [15]. Although there is abundant literature indicating the potential for predicting soil attributes using these techniques in temperate regions [16–19], tropical soils have different characteristics. The high temperature and humidity of the tropics cause severe changes in the mineralogical and biological properties of tropical soils compared to temperate soils; for example, temperate soils typically have more complex mineralogy than tropical soils, and biological activity is significantly higher in tropical soils compared to temperate soils [20]. In addition, most research is concerned with the prediction of the total content of elements in the soil [21,22], rather than their ionic forms and humic fractions, as in this article.

The use of supervised machine learning techniques in soil science has also been growing rapidly due to their use in the creation of statistical models with the goal of "learning" or "understanding" data collected from the soil [16]. Different types of models have been used for the calibration of spectral data with soil data. These include the Partial Least Squares Regression (PLSR) and the Support Vector Machine (SVM) [23].

This research assumes that the Vis-NIR-SWIR and X-ray fluorescence spectroscopy techniques are capable of identifying nitrogen, total organic carbon, and humic fractions in Ferralsols and that the calibration models based on machine learning PLSR and SVM are capable of providing satisfactory values for the attributes under study, considering the specificities of tropical soils.

The objective was to verify the performance of the spectral techniques as well as validation models in the prediction of nitrogen, total organic carbon, and humic fractions under different cultivation conditions.

2. Materials and Methods

2.1. Description of Site and Soil Sampling Procedures

The study area is situated at the Experimental Farm of the University of Oeste Paulista—UNOESTE, in Presidente Bernardes—SP Brazil, with geographical coordinates of South latitude 22°17′13″ and West longitude 51°40′34″. The experiment was established in 2014 and consists of a consortium system composed of the forage *Megathyrsus maximus* cv. Mombasa and the leguminous plants Guandu bean (*Cajanus cajan*) and *Macrotyloma axillare* cv. Java (Figure 1).

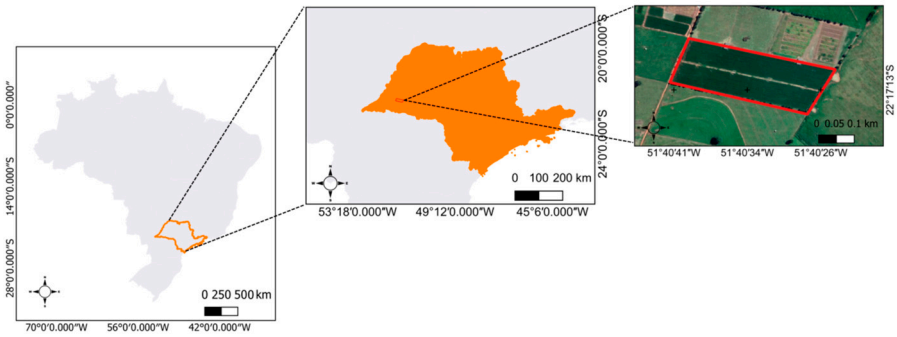

Figure 1. Map of the experimental area located in Brazil.

The soil is classified as Ferralsols, with 17% clay in the 0–10 cm stratum [24] (Table 1), and the regional climate, according to the classification of [25], is of the CWA type, with a mean annual temperature of 25 °C and precipitation in two distinct seasons, the rainy season from October to March and the dry season from April to September.

Table 1. Particle size distribution of soils in the experimental area.

Depth (cm)	Granulometry (g kg^{-1})			Structure Class
	Sandy	Silt	Clay	
0–10	773	48	179	Sandy Middle
10–20	763	68	169	Sandy Middle
20–40	736	41	223	Sandy Middle
40–60	707	63	230	Sandy Middle
60–80	695	55	250	Sandy Middle
80–100	697	56	247	Sandy Middle

2.2. Experiment Design, Management Description and Soil Sampling

The experimental area is structured in a randomized block design with four treatments and four replications: *M. maximus* cv. Mombasa with N fertilizer (200 kg N ha^{-1}) (M+N); *M. maximus* cv. Mombasa without N fertilizer (M-N); *M. maximus* cv. Mombasa in intercropping with Guandu bean (M+G); *M. maximus* in intercropping with cv. Java (M+J). From 2017 to 2021, soybeans and forage were intercropped, aiming to benefit both and improve soil quality. From 2021 onward, the management of the area was carried out only with the maintenance of the *Megathyrsus maximus* cv. Mombasa pasture in the whole area. It should be noted that the whole design has been maintained and that the nitrogen fertilization has been carried out only in the specific areas intended for the mineral fertilization. In the other areas, the pasture was maintained without fertilization. The remaining legume species were used to maintain biological N fixation.

Soil samples were collected with an auger at ten different points in each plot. They were collected at depths of 0–20 and 80–100 cm. A total of 80 samples were collected. Each sample was divided into two portions: 180 g for spectral analysis and 180 g for nitrogen and total organic carbon analysis. The soil contents were stored in a freezer at −15 °C for the determination of inorganic and total nitrogen, total organic carbon, and chemical

fractionation of organic matter. Thus, the inorganic nitrogen content was preserved until the beginning of the laboratory analyses [26].

The plot intended for spectroscopic analysis was dried in a forced ventilated oven at 45 °C for 24 h [26]. The soil samples were sieved through a 2.00 mm mesh (9 mesh) for the Vis-NIR-SWIR spectroradiometer and the XRF spectrometer [27,28].

2.3. Chemical Analysis of the Soil

2.3.1. Determination of Soil Organic Matter and Total Organic C, Chemical Fractionation of Organic Matter, and Quantification of Carbon in Fractions

For the determination of soil organic matter content, 2 g of soil from each sample was sieved through a 0.250 mm (60 mesh) sieve. The procedure was in accordance with the method of [29], adapted from [30]. Humic fractions were extracted using [29] methodology, adapted from [30].

The 1 g of dry soil was placed in 50 mL centrifuge tubes, and 10 mL of NaOH solution (0.1 mol L^{-1}) was pipetted into each tube. The tubes were then vortexed on a vertical shaker at 12 rpm for 1 h and allowed to stand for 24 h. The tubes were centrifuged at 3000 rpm for 20 min after 24 h. The supernatant obtained in this way was transferred to 100 mL beakers. Moreover, 10 mL NaOH (0.1 mol L^{-1}) was pipetted into each tube, shaken, and left for 1 h. Centrifugation at 3000 rpm and removal of the supernatant were repeated.

The alkaline extract contained in the beakers, obtained by removing the supernatant, contains the humic and fulvic fractions, and its pH was adjusted to 2.0 using a 20% H_2SO_4 solution. The residue that remains in the tubes after the removal of the supernatant contains the humine fraction, which is placed in an oven at a temperature of 45 °C for a period of 72 h.

After pH adjustment, the extract containing humic and fulvic acids was transferred to other centrifuge tubes and left for 18 h to completely precipitate the humic fraction. At the end of this period, they were centrifuged at 3000 rpm for 5 min. The resulting supernatant contained the fulvic fraction and was transferred to 50 mL volumetric flasks and volume measured with deionized water. The precipitate at the bottom of the centrifuge tubes, the humic fraction, was diluted and homogenized with 30 mL of NaOH (0.1 mol L^{-1}). It was transferred to 50 mL volumetric flasks, and the volume was made up with NaOH solution (0.1 mol L^{-1}).

(I) Quantify the organic carbon contained in the humic and fulvic fractions:

The 5 mL of humic or fulvic fraction extract was pipetted into 100 mL digestion tubes. A volumetric pipette was used to add 10 mL of $K_2Cr_2O_7$ solution (0.033 mol L^{-1}). This was followed by 10 mL of concentrated H_2SO_4. The tubes were placed in the digestion block at 170 °C. They were kept at this temperature for 30 min.

After cooling to room temperature, 5 drops of ferrous indicator solution were added. The solution was titrated with ammonium ferrous sulfate solution (0.03 mol L^{-1}). The turning point of the titration was clear and went from green to purple and possibly to red.

Under the same conditions, 6 blank controls were prepared. Furthermore, 3 of these were added to the digestion block with the samples, and the other 3 were left unheated at room temperature. The unheated blank controls are important for the calculation of the total loss of dichromate by heating in the absence of a sample.

(II) Quantify the organic carbon contained in the humine fraction:

The 0.5 g of the humine fraction was weighed. It was transferred to the digestion tubes. Moreover, 5 mL of $K_2Cr_2O_7$ (0.167 mol L^{-1}) was added using a volumetric pipette. This was followed by 15 mL of concentrated H_2SO_4. The samples were digested in a digestion block at a temperature of 170 °C and held at this temperature for 30 min. After cooling to room temperature, the contents of each tube were transferred to a 250 mL Erlenmeyer flask. Deionized water was added to make the final volume 80 mL. Moreover, 0.3 mL of indicator solution was added and titrated with ammonia ferrous sulfate (0.1 mol L^{-1}). Blank controls were prepared using the same procedures.

2.3.2. Inorganic Nitrogen Determination

To determine the inorganic forms of N (NH_4^+ and NO_3^-) in soil, 5 cm^3 of soil was taken from each stored sample. Furthermore, 50 mL of 1 mol L^{-1} KCl solution was added. The mixture was stirred for 60 min and decanted for an additional 30 min. An aliquot of 25 mL of the supernatant was transferred to the distillation flask by means of a volumetric pipette.

(I) Determination of the N-NH_4^+ content:

0.2 g of MgO (using a calibrated measure) was added to the flask containing the KCl extract and distilled for about 4 min, collecting about 30 mL of the distillate in a 50 mL beaker with volume graduation and containing 5 mL of boric acid indicator solution.

(II) Determination of the N-NO_3^- content:

After determining N-NH_4^+, 1 mL of the sulfamic acid solution was added to the KCl extract, and the distilling flask was shaken for a few seconds to destroy the N-NO_2^-. The flask was replaced in the distillation apparatus, the Devarda alloy was added, and the distillation was continued until approximately 30 mL of the distillate was collected in a 50 mL beaker containing 5 mL of boric acid indicator solution, in accordance with [31].

2.3.3. Determination of Total Nitrogen Content

From each sample, 1 g of soil was collected and transferred to a digestion tube (Folin–Wu type) for the determination of total soil N. Each set of digestion blocks contains one standard sample and one blank. One gram of the digestion mixture is added to the digestion tube. Dispense the mixture using a spoon-type measure. Moreover, 3.0 mL of concentrated sulfuric acid was added. The tubes were placed in a digester block. The mixture was carefully heated until it stopped foaming. A small glass funnel (25 mm diameter) was placed over the tubes. The temperature was increased and left to boil for five hours (approximately 360 °C) until the contents of the flask became clear. The temperature of the block was adjusted so that H_2SO_4 condensed to about 1/3 of the digester tube height. The tubes were removed from the digester block and allowed to cool down to room temperature according to the procedure described in [31].

2.4. Spectroscopic Analysis of Samples

2.4.1. Visible, Near Infrared, and Shortwave Infrared (Vis-NIR-SWIR)

Analysis was performed according to the method described by [27], where soil samples were dried in a forced-air oven at 45 °C for 24 h. They were then crushed and sieved through a 2 mm mesh sieve (9 mesh). The samples were placed in Petri dishes in 5 g portions, with the sample surface flattened to reduce relief. The spectral data were obtained using a FieldSpec3 spectroradiometer (Analytical Spectral Devices, Boulder, CO, USA) with a wavelength range of 350 to 2500 nm.

2.4.2. X-ray Fluorescence Analysis (XRF)

Analysis was performed according to the method described by [28], where soil samples were dried in a forced-air oven at 45 °C for 24 h and then sieved through 2 mm mesh (9 mesh). An Olympus Delta Professional portable X-ray fluorescence spectrometer (Olympus, Center Valley, PA, USA) with two excitation modes was used for analysis. The instrument has a 50 keV silver X-ray anode and a 2.048-channel silicon drift detector. There are two built-in calibration methods, soil and geochemical, which work independently and read different elements. Soil mode was used to analyze soil samples.

2.5. Analyzing Data

The data were extracted and tabulated in worksheets along with the corresponding chemical analysis data for the determination of N, TOC, and humic fractions. Partial Least Squares Regression (PLSR) and Support Vector Machine (SVM) were used as machine learning algorithms. These algorithms were chosen because of their characteristics in working with the data. PLSR is a linear regression, and SVM is a nonlinear regression [32].

Of the 0–20 cm samples, 70% were randomly selected for training and 30% for model validation. Cross-validation was performed with 5-fold repeatability to avoid overfitting. This statistical process was repeated 50 times. An average of the metric values was generated. For the 80–100 cm soil depth dataset, this process was performed. The algorithms were run using the Caret package and PLS. The method was switched for each algorithm in the RStudio® v. 4.1.3 software.

The relationship between observed and predicted values was evaluated using the coefficient of determination (R^2), root mean square error (RMSE), and interquartile range performance ratio (RPIQ). Models were classified based on R^2 values in accordance with the methodology [33]. Models with $R^2 \geq 0.75$: good models for accurate prediction of soil properties; R^2 0.75 to 0.50: satisfactory models with room for improvement; and $R^2 \leq 0.50$: nonsignificant models without prediction ability.

3. Results

3.1. Validation of PLSR and SVM Prediction Models Using Vis-NIR-SWIR and XRF Spectroscopy on Soil Samples of Mombasa Intercropped with Guandu Beans and Java

3.1.1. Mombasa + Guandu Crop (M+G)

The validation of the PLSR and SVM models for the 0–20 cm soil layers in the M+G cropplot is shown in Figure 2. Adequate coefficients of determination were obtained in the Vis-NIR-SWIR spectral region for fulvic acid (R^2 0.72) and humic acid (R^2 0.83) in the PLSR model (Figure 2a). At the XRF energy level, coefficients of determination were obtained for ammonium (R^2 0.56) and total organic carbon (R^2 0.73) (Figure 2a). For the SVM model (Figure 2b), the Vis-NIR-SWIR wavelength showed a satisfactory coefficient only for the fulvic acid (R^2 0.54). XRFs gave good results for ammonium (R^2 0.66) and total organic carbon (R^2 0.69).

In the 80–100 cm layer (Figure 3), the PLSR model yielded coefficients of determination in the Vis-NIR-SWIR spectral range for ammonium (R^2 0.73), nitrate (R^2 0.69), total nitrogen (R^2 0.78), total organic carbon (R^2 0.56), fulvic acid (R^2 0.65), and humic acid (R^2 0.92) (Figure 3a). For XRF, the coefficients of determination were for nitrate (R^2 0.85), total nitrogen (R^2 0.54), total organic carbon (R^2 0.88), fulvic acid (R^2 0.97), and humic acid (R^2 0.69) (Figure 3a). In the SVM model (Figure 3b), the Vis-NIR-SWIR wavelength showed satisfactory and reasonable coefficients of determination for ammonium (R^2 0.58), nitrate (R^2 0.64), total nitrogen (R^2 0.71), total organic carbon (R^2 0.70), fulvic acid (R^2 0.78) and humic acid (R^2 0.60). In XRF, the model generated coefficients for nitrate (R^2 0.86), total organic carbon (R^2 0.88), fulvic acid (R^2 0.99), and humic acid (R^2 0.60).

3.1.2. Mombasa + Java Crop (M+J)

Validation of PLSR and SVM models for 0–20 cm soil layer in M+J plot is shown in (Figure 4). The PLSR model gave satisfactory results in Vis-NIR-SWIR for ammonium (R^2 0.62), nitrate (R^2 0.74), fulvic acid (R^2 0.58) and humic acid (R^2 0.73) (Figure 4a). In the XRF analysis, only the humine fraction showed a valid result (R^2 0.65) (Figure 4a). For the SVM model, only the nitrate (R^2 0.70) and humic acid (R^2 0.67) fractions were valid in Vis-NIR-SWIR (Figure 4b).

In the 80–100 cm layer (Figure 5), the PLSR model at the Vis-NIR-SWIR wavelength gave adequate results for ammonium (R^2 0.73), nitrate (R^2 0.62), total nitrogen (R^2 0.60), total organic carbon (R^2 0.73), and humine (R^2 0.86) (Figure 5a). In XRF, the results were satisfactory for ammonium (R^2 0.85), nitrate (R^2 0.72), total nitrogen (R^2 0.59), total organic carbon (R^2 0.99), humic (R^2 0.60), and humine (R^2 0.99) (Figure 5a). In the SVM model, Vis-NIR-SWIR spectroscopy showed valid coefficients of determination for ammonium (R^2 0.85), nitrate (R^2 0.72), total nitrogen (R^2 0.68), total organic carbon (R^2 0.74), humic acid (R^2 0.87), and humine (R^2 0.94) (Figure 5b). The XRF results were ammonium (R^2 0.84), total nitrogen (R^2 0.59), total organic carbon (R^2 0.99), fulvic acid (R^2 0.50), humic acid (R^2 0.58), and humine (R^2 0.51) (Figure 5b).

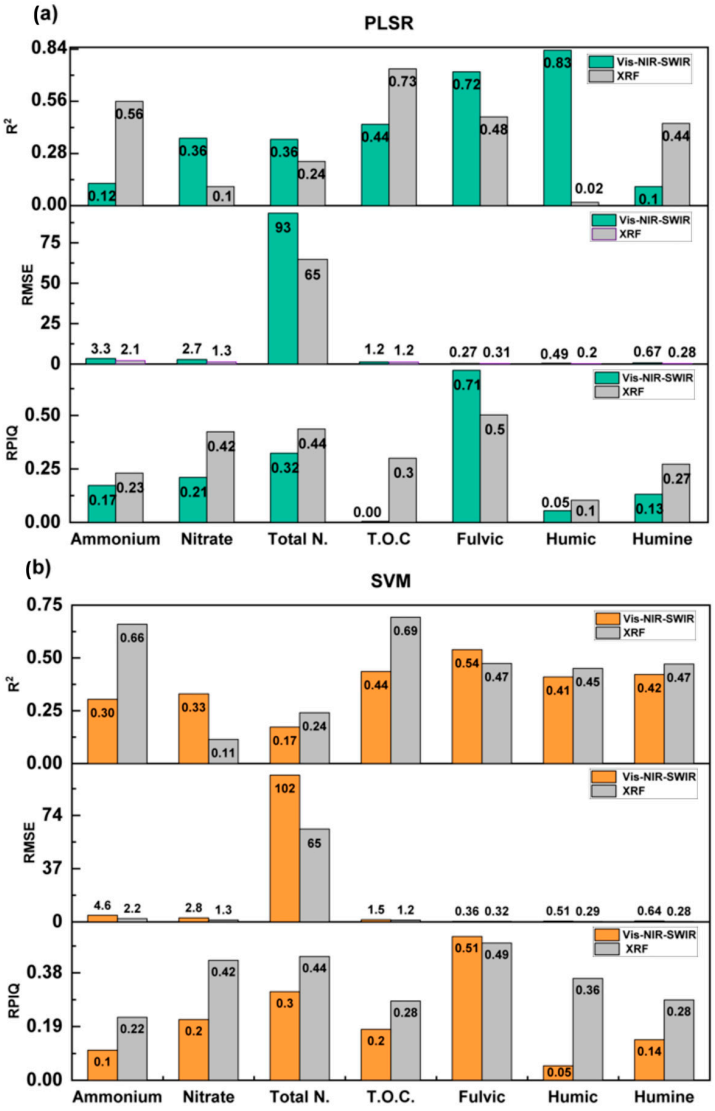

Figure 2. Performance metrics of prediction models: (**a**) PLSR and (**b**) SVM applied to samples from the Mombasa + Guandu plot, 0–20 cm soil layer.

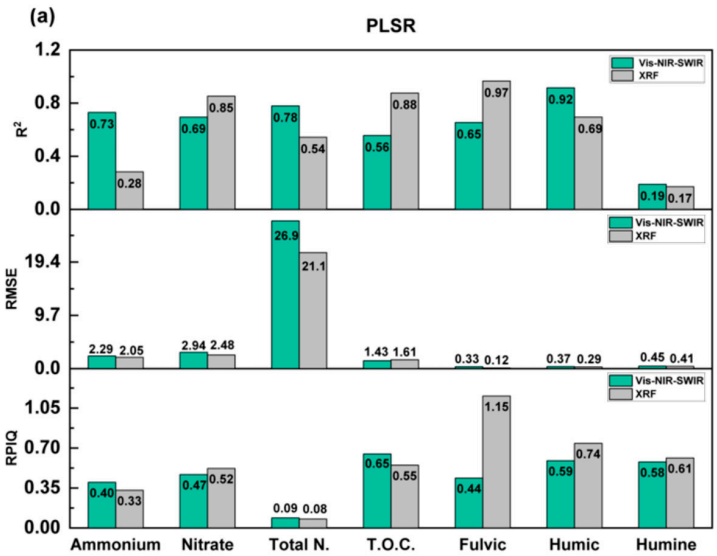

Figure 3. *Cont*.

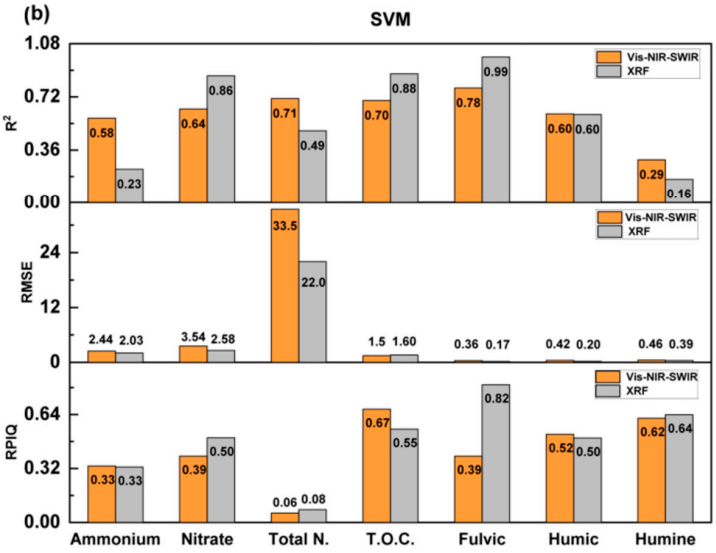

Figure 3. Performance metrics of prediction models: (**a**) PLSR and (**b**) SVM applied to samples from the Mombasa + Guandu plot, 80–100 cm soil layer.

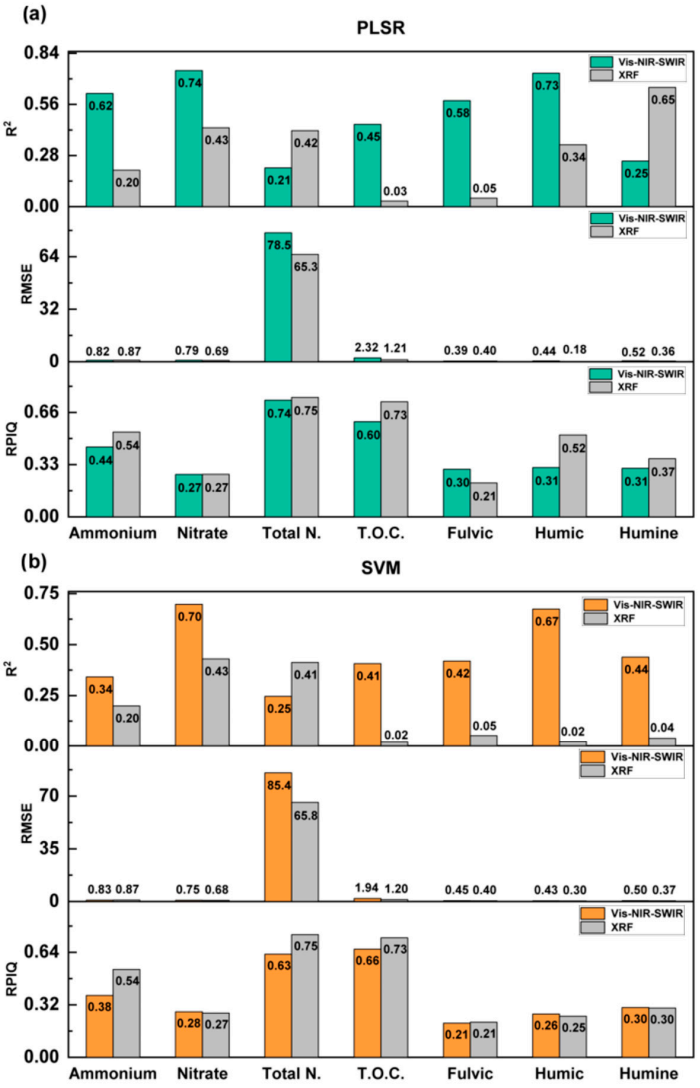

Figure 4. Performance metrics of prediction models: (**a**) PLSR and (**b**) SVM applied to samples from the Mombasa + Java plot, 0–20 cm soil layer.

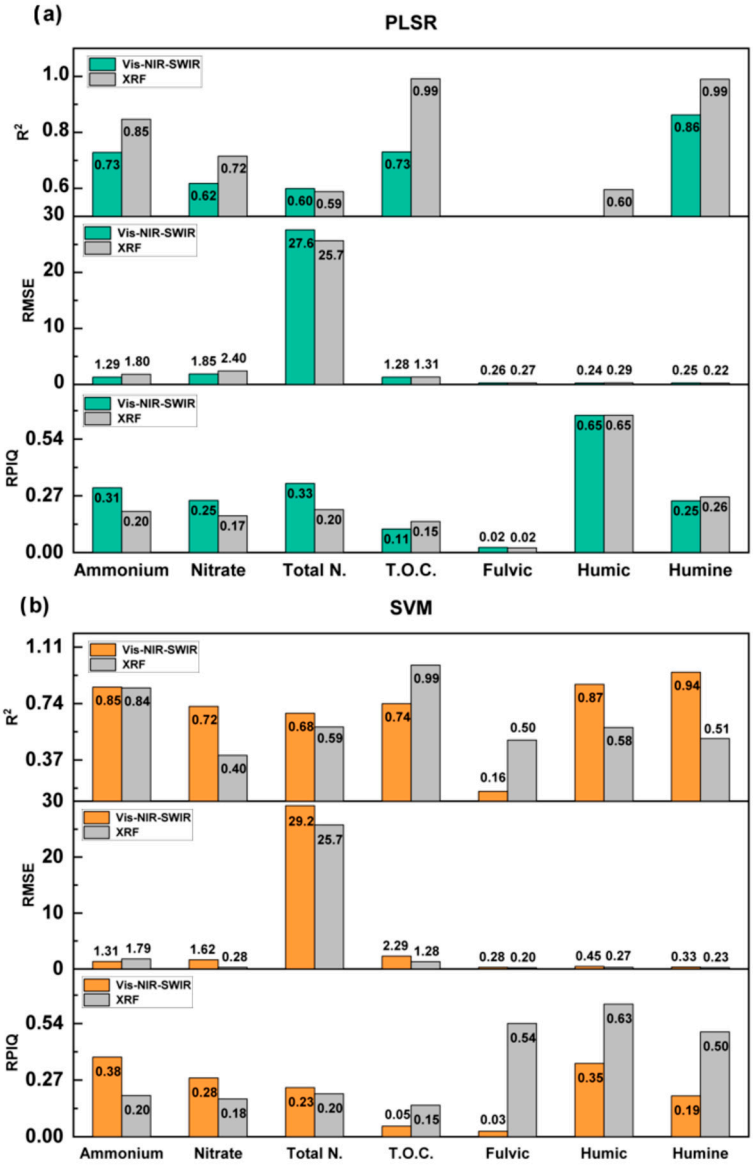

Figure 5. Performance metrics of prediction models: (**a**) PLSR and (**b**) SVM applied to samples from the Mombasa + Java plot, 80–100 cm soil layer.

3.1.3. Mombasa Crop with Mineral Nitrogen Fertilization (M+N)

The validation of the PLSR and SVM models for the 0–20 cm soil layer in the M+N is presented in Figure 6. The PLSR model showed satisfactory results at the Vis-NIR-SWIR wavelength with total organic carbon (R^2 0.69), fulvic acid (R^2 0.51), and humic acid (R^2 0.64) (Figure 6a). In XRF, ammonium (R^2 0.89), total nitrogen (R^2 0.72), and humine (R^2 0.75) (Figure 6a). The SVM model (Figure 6b) showed high coefficients of determination for ammonium (R^2 0.68), fulvic (R^2 0.73), and humic acids (R^2 0.56) with the Vis-NIR-SWIR spectroscopic technique. The XRF results were excellent for ammonium (R^2 0.79), total nitrogen (R^2 0.71), and humine (R^2 0.81) (Figure 6b).

For the 80–100 cm layer, in the PLSR model, the Vis-NIR-SWIR wavelength showed satisfactory results only for nitrate (R^2 0.86) and total organic carbon (R^2 0.68) (Figure 7a). In XRF, for ammonium (R^2 0.64), nitrate (R^2 0.54), and total organic carbon (R^2 0.52) (Figure 7a). Using the SVM model (Figure 7b), Vis-NIR-SWIR showed satisfactory coefficients of determination only for nitrate (R^2 0.73) and total organic carbon (R^2 0.58). XRF only ammonium (R^2 0.67) and nitrate (R^2 0.56) (Figure 7b).

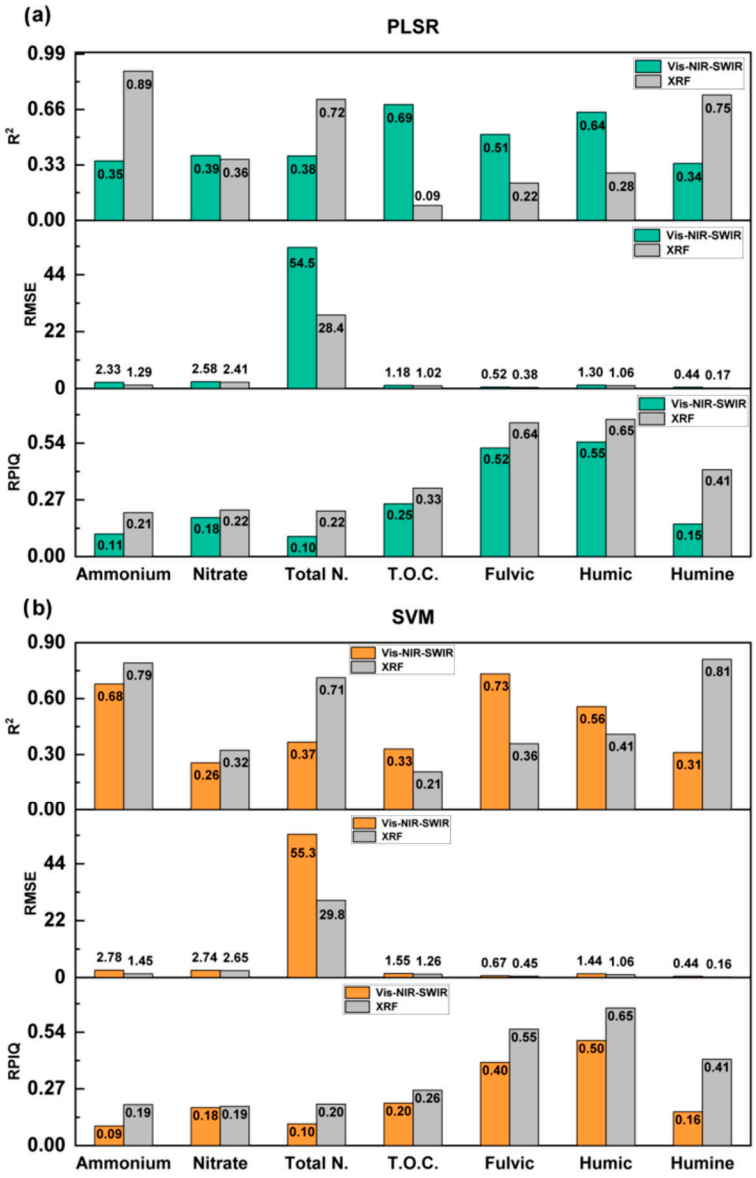

Figure 6. Performance metrics of prediction models: (**a**) PLSR and (**b**) SVM applied to samples from the Mombasa + Nitrogen plot, 0–20 cm soil layer.

3.1.4. Mombasa Crop without Nitrogen Fertilization (M-N)

Validation of PLSR and SVM models for the 0–20 cm layer in M-N is shown in (Figure 8). The PLSR model showed satisfactory coefficients at the Vis-NIR-SWIR wavelength for ammonium (R^2 0.54), fulvic acid (R^2 0.57), and humic acid (R^2 0.74) (Figure 8a). In the XRF, for ammonium (R^2 0.86), total nitrogen (R^2 0.76), fulvic acid (R^2 0.86), and humic (R^2 0.66) (Figure 8a). In the SVM model (Figure 8b), Vis-NIR-SWIR gave satisfactory values for total nitrogen (R^2 0.63) and humic acid (R^2 0.58). By XRF, for ammonium (R^2 0.79), total nitrogen (R^2 0.73), fulvic acid (R^2 0.83), and humic (R^2 0.67) (Figure 8b).

At the 80–100 cm layer (Figure 9a), the PLSR model in Vis-NIR-SWIR exhibited satisfactory coefficients of determination for ammonium (R^2 0.60), total organic carbon (R^2 0.69), and humine (R^2 0.61). For XRF, ammonium (R^2 0.80), nitrate (R^2 0.50), and total organic carbon (R^2 0.62) (Figure 9a). SVM model (Figure 9b), Vis-NIR-SWIR only satisfactory results for total organic carbon (R^2 0.55) and humine (R^2 0.67). In XRF, for ammonium (R^2 0.85), nitrate (R^2 0.52), and total organic carbon (R^2 0.68) (Figure 9b).

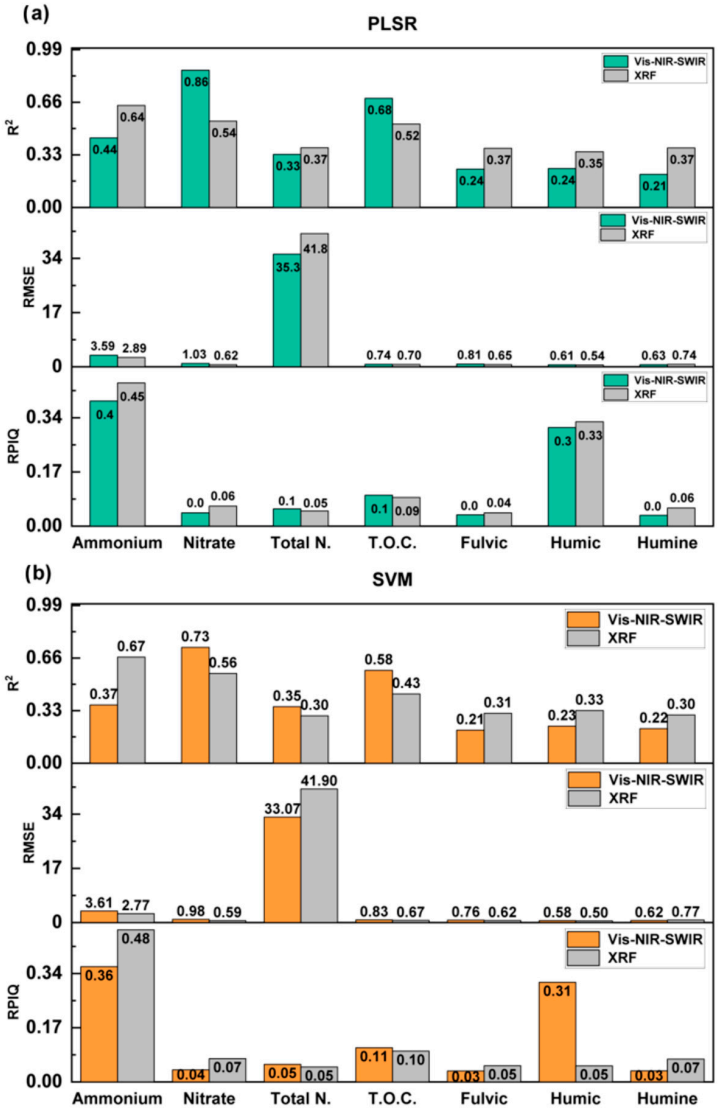

Figure 7. Performance metrics of prediction models: (**a**) PLSR and (**b**) SVM applied to samples from the Mombasa + Nitrogen plot, 80–100 cm soil layer.

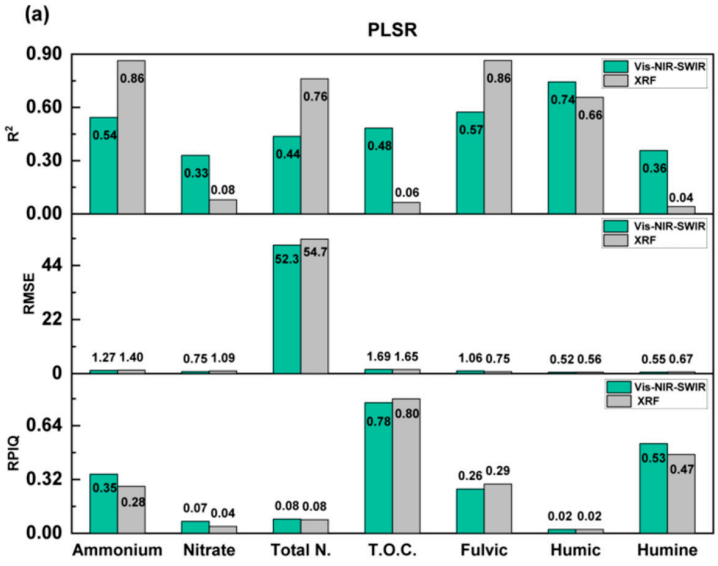

Figure 8. *Cont.*

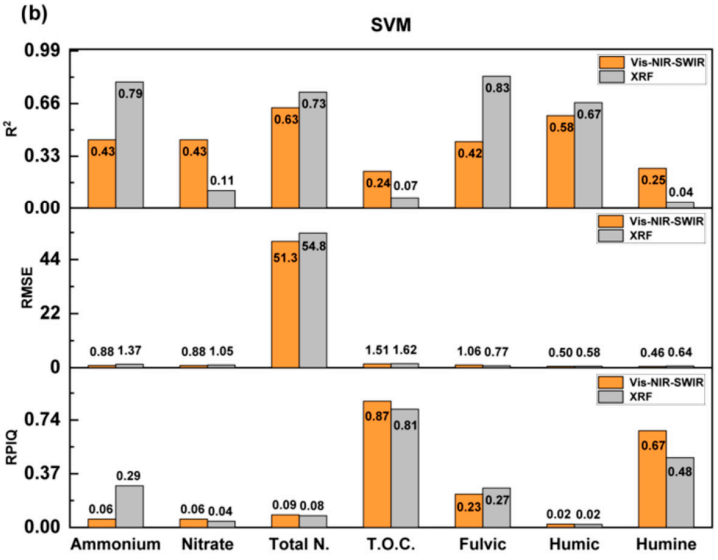

Figure 8. Performance metrics of prediction models: (**a**) PLSR and (**b**) SVM applied to samples from the Mombasa—Nitrogen plot, 0–20 cm soil layer.

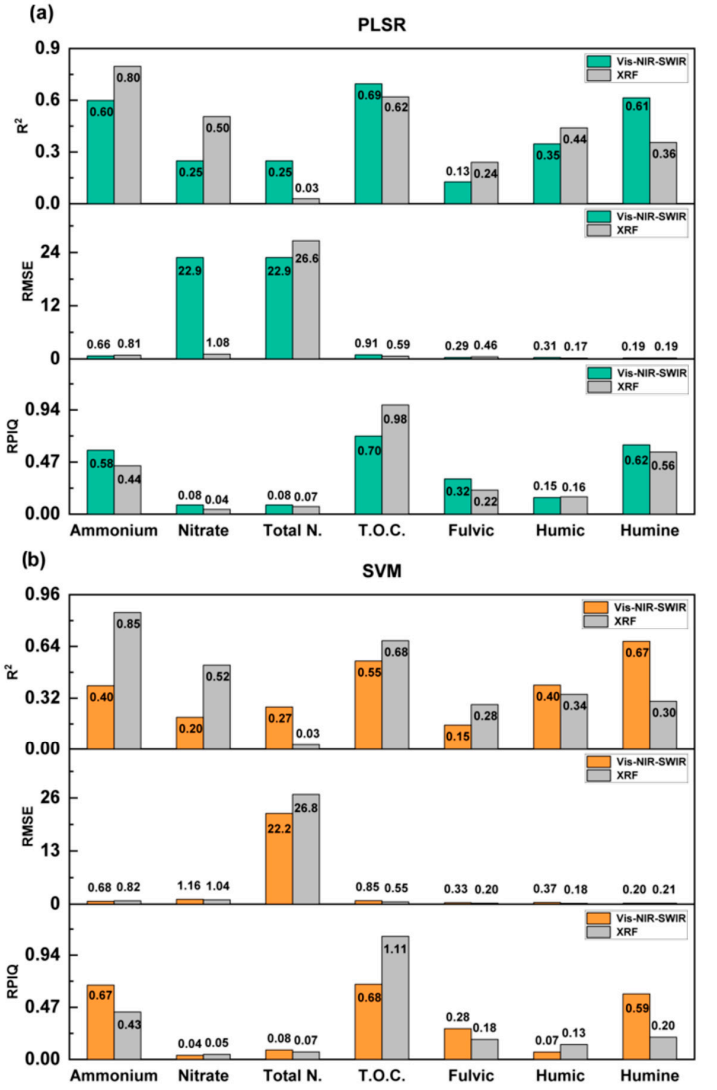

Figure 9. Performance metrics of prediction models: (**a**) PLSR and (**b**) SVM applied to samples from the Mombasa—Nitrogen plot, 80–100 cm soil layer.

4. Discussion

In the 0–20 cm soil layer of the M+G system (Figure 2a), it was observed that the Vis-NIR-SWIR spectral response of the PLSR model gave adequate coefficients of determination for fulvic acid (R^2 0.72) and humic acid (R^2 0.83). Similar results were found in [34] when the PLSR model was validated, with R^2 0.78 for fulvic acid and R^2 0.80 for humic acid. Changes in soil management are a relevant issue contributing to the increase in carbon fractions, according to [35].

XRF showed satisfactory results with ammonium (R^2 0.56) and total organic carbon (R^2 0.73) (Figure 2a). In a study [36], coefficients of determination of R^2 0.60 were obtained using the XRF spectrum in combination with PLS regression to predict total organic carbon content. The combined planting of grasses and legumes has shown good results in soil conservation [37], and it contributes to N storage through biological fixation [38]. This intercropping system is also capable of improving soil total organic carbon accumulation [39].

In the SVM model, the spectral response of Vis-NIR-SWIR and XRF showed slightly lower determination coefficients for organic attributes fulvic acid and total organic carbon (Figure 2b) in comparison to the PLSR model. A similar situation was reported by [40]. They used Vis-NIR to predict total organic carbon in the 0–30 cm soil layer. The PLSR model showed an R^2 of 0.63, while the SVM model showed an R^2 of 0.30. For the 80–100 cm layer (Figure 3), practically all attributes were validated. In the PLSR model (Figure 3 a), the Vis-NIR-SWIR spectrum showed satisfactory and adequate results for ammonium (R^2 0.73), nitrate (R^2 0.69), total nitrogen (R^2 0.78), total organic carbon (R^2 0.56), fulvic acid (R^2 0.65), and humic acid (R^2 0.92). The nitrogen compounds ammonium, nitrate, and total nitrogen stood out. Using Vis-NIR-SWIR in a PLSR model, the authors [41] obtained R^2 0.83 for total nitrogen. Legumes are natural sources of nitrogen [42] through atmospheric nitrogen fixation to the soil in a symbiotic manner, as a result of the interaction between the legume and the rhizobium (*Bradyrhizobium* spp.) [43].

The predictions of ammonium and nitrate were superior to the results obtained with Vis-NIR-SWIR in the SVM model (Figure 3b). In a study by [44] on the prediction of ammonium, nitrate, and urea in soil using NIR, they reported that the accuracy of ammonium and nitrate detection by the PLSR model was superior to that of the SVM model. In terms of XRF wavelength, both the PLSR model and the SVM model showed the same validation capability (Figure 3a,b). The exception was the prediction of total nitrogen in the PLSR model (Figure 3a), which was absent in the SVM (Figure 3b). A similar result was obtained by [45], validating R^2 of 0.50 for total nitrogen using the PLSR model. Although the XRF spectrometer does not directly determine these attributes, other studies have reported the ability to determine them by elemental association [46–48]. According to [49], XRF is highly dependent on the atomic number of the elements. Due to their low emission energies, light elements, elements with atomic numbers below 12, are difficult to determine.

The PLSR model showed satisfactory and adequate results in the 0–20 cm soil layer of the M+J crop (Figure 4). The authors [44] obtained an R^2 of 0.88 for ammonium. This result is superior to the SVM model. Another study [50] obtained a coefficient of determination of 0.82 using the PLSR model to evaluate the nitrate content in the soil. Organic matter derived from cultivated crops not only contributes to N accumulation in plant biomass [51]. It consists of 80–90% humic fractions [52], called fulvic acids, humic acids, and the humine fraction [53]. These fractions have a high capacity to store carbon in the soil [54] and reflect the ability of the soil to remain healthy and productive in the long term [53].

In the SVM model, only Vis-NIR-SWIR spectroscopy produced results (Figure 4b). This model has often been applied to Vis-NIR spectral datasets [55]. In some studies, it has produced more accurate calibration results than the PLSR method [32]. However, the estimation capacity and computational efficiency of the SVM model can be reduced by possible redundancies in the data, such as collinearity between them, and sometimes by the noise contained in the spectral data [56]. This information may explain the poor

performance of the SVM model on Vis-NIR-SWIR and even XRF spectral responses over PLSR model results (Figure 4b).

In the 80–100 cm layer, the PLSR model at the Vis-NIR-SWIR wavelength showed satisfactory results for ammonium (R^2 0.73), nitrate (R^2 0.62), total nitrogen (R^2 0.60), total organic carbon (R^2 0.73), and humine (R^2 0.86) (Figure 5a). Legume cropping systems have many benefits for soil fertility. They increase organic carbon, humic fractions, and the availability of nitrogen and phosphorus [57].

XRF spectral response showed satisfactory determination coefficients for ammonium (R^2 0.85), nitrate (R^2 0.62), total nitrogen (R^2 0.59), and especially total organic carbon (R^2 0.99) and humine (R^2 0.99) (Figure 5a). In addition, fluorescence spectroscopy can be a complementary method to reflectance spectroscopy [58]. The fluorescence technique is the measurement of the photoluminescence of molecules that emit light when they absorb electromagnetic energy [59]. This may be the reason for the high performance of the validation results for total organic carbon and humic fractions.

The SVM model in the 80–100 cm layer (Figure 5b) showed slightly better predictive results for Vis-NIR-SWIR and XRF than the PLSR model. The authors [60] obtained SVM results that were superior to the PLSR model, with ammonium showing an R^2 of 0.70, nitrate (R^2 0.82), and total nitrogen (R^2 0.94). Because it successfully models the linear relationship between spectral data and chemical data, the PLSR method developed by [61] has become the most widely used calibration method for estimating organic carbon and organic matter compounds [62]. However, nonlinearity between spectral and chemical data is common. It is usually caused by variations in the instruments used for spectral measurements, such as lamp fading or sensor sensitivity [63], and especially by heterogeneous soil characteristics [64]. Therefore, nonlinear methods such as support vector machine (SVM) regression can sometimes provide better results than linear methods [65].

In the 0–20 cm soil layer of the M+N crop, the Vis-NIR-SWIR spectral response in the PLSR model was for total organic carbon (R^2 0.69) and fulvic (R^2 0.51) and humic (R^2 0.64) acid (Figure 6a). In a study by [66] that modeled total organic carbon using Vis-NIR in the 0–30 cm soil layer, they found total organic carbon (R^2 0.86) and recalcitrant carbon (more stable carbon fraction with low decomposability such as fulvic and humic acids) of (R^2 0.82) in the PLSR, which outperformed the other models. Quantifying the soil organic carbon compartments helps us understand how stable forms of C are being conserved or lost in the soil, given current climate variability [66].

XRF gave good results for ammonium (R^2 0.89), total nitrogen (R^2 0.72), and humine (R^2 0.75) (Figure 6a). Satisfactory results were also obtained by [67] with total nitrogen (R^2 0.50) and soil organic matter (R^2 0.56), using the random forest model. The application of mineral nitrogen fertilizers is one of the most important management tools for the maintenance and the increase in the productivity of the agricultural systems [68].

In the SVM model, the Vis-NIR-SWIR spectral response was satisfactory for ammonium (R^2 0.68), fulvic acid (R^2 0.73), and humic acid (R^2 0.56) (Figure 6b). In a study by [69] evaluating forest soil properties for studying humus using Vis-NIR, they found R^2 0.71 for total nitrogen and R^2 0.72 for total organic carbon in the SVM model. In XRF, humine (R^2 0.81) stood out (Figure 6b). For the development of management strategies, the availability of nutrients in the soil is the basis for making confident decisions. Therefore, it is necessary to update and complement the current methods for the quantification of the humic properties of soils [69].

For the 80–100 cm layer, in the PLSR model, the Vis-NIR-SWIR spectral response was only present for nitrate (R^2 0.86) and total organic carbon (R^2 0.68) (Figure 7a). Authors [70] obtained R^2 0.89 for total nitrogen and R^2 0.75 for soil organic matter using the PLSR model. The process of nitrogen mineralization in the soil is considered a critical point of fertility. It is relevant for the supply and evaluation of the content of N readily assimilable by plants. However, if not carefully managed, the mineral N content in the soil can exceed the crop needs, and then the remaining nitrate will lead to increased leaching along the soil profile [71]. XRF values were obtained for ammonium (R^2 0.64), nitrate (R^2 0.54) and total

organic carbon (R^2 0.52) (Figure 7a). Sandy soils are more susceptible to NO_3^- leaching than clay soils [72]. Therefore, determining the different types of N present in soils is of great value for agricultural production [44].

The SVM model results (Figure 7b) were not very different from those obtained with the PLSR model (Figure 7a). In a recent study by [73], where carbonates and organics were characterized by reflected energy, they obtained good results with the PLSR and SVM models, with R^2 0.84 and R^2 0.85 for organics and R^2 0.77 and R^2 0.78 for carbonates, respectively. However, the strategic use of nitrogen fertilizer in precision agriculture can be guided by the effective and accurate quantification of N and organic matter content in agricultural soils [44].

In the 0–20 cm layer of the M-N crop, the Vis-NIR-SWIR wavelength of the PLSR model showed satisfactory coefficients for ammonium (R^2 0.54), fulvic acid (R^2 0.57), and humic acid (R^2 0.74) (Figure 8a). The authors [74] measured the carbon content of microbial biomass using NIR spectroscopy and obtained an R^2 of 0.57 using the PLSR model. Nitrogen is one of the most limiting nutrients for the growth and development of plants. In systems where this nutrient is lacking, the native soil microorganisms take over this role and make the nutrients available through mineralization processes [75]. XRF validation results were satisfactory for ammonium (R^2 0.86), total nitrogen (R^2 0.76), fulvic acid (R^2 0.86), and humic acid (R^2 0.66) (Figure 8a). Fulvic and humic acid fractions are important components of soil. They improve aggregates and soil fertility and reduce soil acidity and alkalinity [76].

In the SVM model, Vis-NIR-SWIR showed satisfactory results for total nitrogen (R^2 0.63) and humic acid (R^2 0.58) (Figure 8b). XRF showed good results for ammonium (R^2 0.79), total nitrogen (R^2 0.73), fulvic acid (R^2 0.83), and humic acid (R^2 0.67) (Figure 8b). Properly managed pasture systems can promote soil benefits such as organic matter accumulation, water retention, nutrient cycling, and increases in total soil carbon stocks [77]. Quantification of soil carbon stock and nitrogen content, which are important components of organic matter, allows understanding of the effects of management on cropping systems [78].

For the 80–100 cm soil layer, the PLSR model showed satisfactory coefficients of determination for the Vis-NIR-SWIR wavelength, with ammonium (R^2 0.60), total organic carbon (R^2 0.69), and humine (R^2 0.61) (Figure 9a). XRF values were ammonium (R^2 0.80), nitrate (R^2 0.50), and total organic carbon (R^2 0.62) (Figure 9a). Belowground biomass is of great importance for carbon and nutrient cycling [79], accounting for more than 80% of the total biomass in pastures. According to [80], the root biomass expresses positive correlations with the stable fractions of organic C (fulvic acid, humic acid, and humine) in the Brazilian pasture soil.

In the SVM model, good results were obtained both for Vis-NIR-SWIR, with satisfactory results for total organic carbon (R^2 0.55) and humine (R^2 0.67) (Figure 9b), and for XRF, with ammonium (R^2 0.85) and nitrate (R^2 0.52) (Figure 9b). Tropical grass cultivation contributes to widening soil pathways by increasing root biomass production, which facilitates carbon uptake and benefits soil carbon cycling [81].

Good soil quality is not only a question of the vitality and productivity of plants but also of the integrity of the agroecosystem as a whole. Healthy soil is the basis for biological communities that support biological diversity, which benefits both the agricultural land and the environment [82].

5. Conclusions

The Vis-NIR-SWIR and XRF spectroscopic techniques showed high performance and are indicated for the prediction of nitrogen, total organic carbon, and humic fractions in Ferralsols of medium sandy texture. However, it is important to highlight that each technique has its own characteristic mechanism of action: Vis-NIR-SWIR detects the element based on harmonic tones, while XRF is based on the atomic number of the element or elemental association.

The PLSR and SVM models showed excellent validation results, allowing them to fit the experimental data, emphasizing that they are different statistical methods.

Author Contributions: Conceptualization, J.A.M.D., M.R.N., C.H.d.S. and C.S.T.; methodology, J.A.M.D. and M.R.N.; software, R.R.P. and J.A.M.D.; formal analysis, B.C.d.L., J.A.M.D., R.F., C.A.d.O., N.G.V., G.Z. and A.S.R.; investigation, B.C.d.L.; resources, B.C.d.L. and J.A.M.D.; writing—original draft preparation, B.C.d.L.; writing—review and editing, B.C.d.L.; supervision, J.A.M.D., M.R.N., C.H.d.S. and C.S.T.; validation, B.C.d.L. and J.A.M.D.; funding acquisition, M.R.N. All authors have read and agreed to the published version of the manuscript.

Funding: This research was funded by "Foundation Coordination for the Improvement of Higher Education Personnel, grant number 001-CAPES/Brazil", and APC was financed by Marcos R. Nanni by "Foundation Araucária, grant number CP03/2021".

Data Availability Statement: The original contributions presented in the study are included in the article, further inquiries can be directed to the corresponding author.

Acknowledgments: We would like to thank the national institutions that support and encourage Brazilian research, CAPES, CNPq, and Fundação Araucária, as well as the higher education institutions, Universidade do Oeste Paulista (Unoeste), the research group Geotechnology in Soil Science (GeoCiS) at the Escola Superior de Agricultura Luiz de Queiroz (Esalq/USP), and the State University of Maringá.

Conflicts of Interest: The authors declare no conflicts of interest.

References

1. Silva, M.A.; Nascente, A.S.; de Mello Frasca, L.L.; Rezende, C.C.; Ferreira, E.A.S.; Filippi, M.C.C.; Lanna, A.C.; Ferreira, E.P.B.; Lacerda, M.C. Plantas de cobertura isoladas e em mix para a melhoria da qualidade do solo e das culturas comerciais no Cerrado. *Res. Soc. Dev.* **2021**, *10*, e11101220008. [CrossRef]
2. Tiecher, T.; Gubiani, E.; Santanna, M.A.; Veloso, M.G.; Calegari, A.; Canalli, B.S.; Finckh, M.R.; Caner, L.; Rheinheimer, D.S. Effect of 26 years of soil tillage systems and winter cover crops on C and N stocks in a Southern Brazilian Oxisol. *Rev. Bras. Ciência Solo.* **2020**, *44*, e0200029. [CrossRef]
3. Soil Survey Staff. *Keys to Soil Taxonomy*, 13th ed.; USDA Natural Resources Conservation Service: Washington, DC, USA, 2022.
4. Oorts, K.; Vanlauwe, B.; Merckx, R. Cation exchange capacities of soil organic matter fractions in a Ferric Lixisol with different organic matter inputs. *Agric. Ecosyst. Environ.* **2003**, *100*, 161–171. [CrossRef]
5. Batista, K.; Vilela, L.A.F. Tropical Grasses—Annual crop intercropping and adequate nitrogen supply increases soil microbial carbon and nitrogen. *Agronomy* **2023**, *13*, 1275. [CrossRef]
6. Lithourgidis, A.S.; Dordas, C.A.; Damalas, C.A.; Damalas, C.A.; Vlachostergios, D.N. An alternative pathway for sustainable agriculture. *Aust. J. Crop. Sci.* **2011**, *5*, 396–410.
7. Dinesh, R.; Suryanarayana, M.A.; Chaudhuri, S.G.; Sheeja, T.E.; Shiva, K.N. Long-term effects of leguminous cover crops on biochemical biological properties in the organic mineral layers of soils of a coconut plantation. *Eur. J. Soil. Biol.* **2006**, *42*, 147–157. [CrossRef]
8. Pietroski, M.; Oliveira, R.; Caione, G. Adubação foliar de nitrogênio em capim Mombaça (*Panicum maximus* cv. Mombaça). *Rev. Agric. Neotrop.* **2015**, *2*, 49–53. [CrossRef]
9. Souza, É.M.; Isepon, O.J.; Alves, J.B.; Bastos, J.F.P.; Lima, R.C. Efeitos da irrigação e adubação nitrogenada sobre a massa de forragem de cultivares de Panicum maximum Jacq. *Rev. Bras. Zootec.* **2005**, *34*, 1146–1155. [CrossRef]
10. Batista, K.; Giacomini, A.A.; Gerdes, L.; Mattos, W.T.; Otsuk, I.P. Impacts of the nitrogen application on productivity and nutrient concentrations of the corn-Congo grass intercropping system in the dry season. *Acta Agric. Scand. Sect. Soil. Plant Sci.* **2019**, *69*, 567–577. [CrossRef]
11. Ladha, J.K.; Peoples, M.B.; Reddy, P.M.; Biswas, J.C.; Bennett, A.; Jate, M.; Krupnik, T.J. Biological nitrogen fixation prospects for ecological intensification in cereal-based cropping systems. *Field Crop. Res.* **2022**, *283*, 108541. [CrossRef]
12. Lai, H.; Gao, F.; Su, H.; Zheng, P.; Li, Y.; Yao, H. Nitrogen distribution and soil microbial community characteristics in a legume–cereal intercropping system: A review. *Agronomy* **2022**, *12*, 1900. [CrossRef]
13. Ng, W.; Anggria, L.; Siregar, A.F.; Hartatik, W.; Sulaeman, Y.; Jones, E.; Minasny, B. Developing a soil spectral library using a low-cost NIR spectrometer for precision fertilization in Indonesia. *Geoderma* **2020**, *22*, e00319. [CrossRef]
14. Pandey, S.; Bhatta, N.P.; Paudel, P.; Pariyar, R.; Hari, M.K.; Khadka, J.; Thapa, T.B.; Rijal, B.; Panday, D. Improving fertilizer recommendations for Nepalese farmers with the help of a soil-testing mobile van. *J. Crop. Improv.* **2018**, *32*, 19–32. [CrossRef]
15. Tavares, T.R.; Molin, J.P.; Javadi, S.H.; Carvalho, H.W.P.; Mouazen, A.M. Combined use of Vis-NIR and XRF sensors for tropical soil fertility analysis: Assessing different data fusion approaches. *Sensors* **2020**, *21*, 148. [CrossRef] [PubMed]
16. AbdulMunnaf, M.; Nawar, S.; Mouazen, A.M. Estimation of secondary soil properties by fusion of laboratory and online measured Vis–NIR spectra. *Remote Sens.* **2019**, *11*, 2819. [CrossRef]

17. Nawar, S.; Buddenbaum, H.; Colina, J.; Kozak, J.; Mouazen, A.M. Estimating the soil clay content and organic matter by means of different calibration methods of vis-NIR diffuse reflectance spectroscopy. *Soil. Tillage Res.* **2016**, *155*, 510–522. [CrossRef]
18. Javadi, S.H.; AbdulMunnaf, M.; Mouazen, A.M. Fusion of Vis-NIR and XRF spectra for estimation of key soil atributes. *Geoderma* **2021**, *385*, 114851. [CrossRef]
19. Kandpal, L.M.; Munnaf, M.A.; Cruz, C.; Mouazen, A.M. Spectra fusion of Mid-Infrared (MIR) and X-ray Fluorescence (XRF) spectroscopy for estimation of selected soil fertility atributes. *Sensors* **2022**, *22*, 34–59. [CrossRef] [PubMed]
20. Hartemink, A.E. Soil science in tropical and temperate regions—Some differences and similarities. *Adv. Agron.* **2002**, *77*, 269–292.
21. Tavares, T.R.; Almeida, E.; Pinheiro Junior, C.R.; Guerreiro, A.; Fiorio, P.R.; Carvalho, H.W.P. Analysis of total soil nutrient content with X-ray Fluorescence spectroscopy (XRF): Assessing different predictive modeling strategies and auxiliary variables. *AgriEngineering* **2023**, *5*, 680–697. [CrossRef]
22. Song, J.; Shi, X.; Wang, H.; Lv, X.; Zhang, W.; Wang, J.; Li, T.; Li, W. Combination of feature selection and geographical stratification increases the soil total nitrogen estimation accuracy based on vis-NIR and pXRF spectral fusion. *Comp. and Eletronics Agrc.* **2024**, *218*, 108636. [CrossRef]
23. McBratney, A.; Gruijter, J.; Bryce, A. Pedometrics timeline. *Geoderma* **2019**, *338*, 568–575. [CrossRef]
24. Embrapa. *Sistema Brasileiro de Classificação de Solos*, 5th ed.; Embrapa: Brasília, Brazil, 2018.
25. Köppen, W.; Geiger, R. Klimate der Erde. Gotha, Verlag Justus Perthes Wall-map 150 cm × 200 cm. *Am. J. Plant Sci.* **1928**, *8*, 91–102.
26. Mattos Junior, D.; Cantarella, H.; Raij, B. Manuseio e conservação de amostras de solo para preservação do nitrogênio inorgânico. *Rev. Bras. Ciênc. Solo* **1995**, *19*, 423–431.
27. Bellinaso, H.; Demattê, J.A.M.; Romeiro, A.S. Soil spectral library and its use in soil classification. *Rev. Bras. Ciênc. Solo* **2010**, *34*, 861–870. [CrossRef]
28. Rosin, N.A.; Demattê, J.A.M.; Leite, M.C.A.; Carvalho, H.W.P.; Costa, A.C.; Greschuk, L.T.; Curi, N.; Silva, S.H.G. The fundamental of the effects of water, organic matter, and iron forms on the pXRF information in soil analyses. *Catena* **2022**, *210*, 105868. [CrossRef]
29. Matos, E.S.; Mendonça, E.S.; Morales, M.M.; Silva, B.R. Carbono total e frações químicas de cabono do solo. In *Matéria Orgânica do Solo—Métodos de Análises*, 2nd ed.; Mendoça, E.S., Matos, E.S., Eds.; Embrapa: Brasília, Brazil, 2017; p. 221.
30. Yeomans, J.C.; Bremner, J.M.A. A rapid and precise method for routine determination of organic carbon in soil. *Soil. Sci. Plant Anal.* **1988**, *19*, 1467–1476. [CrossRef]
31. Cantarella, H.; Trivelin, P.C.O. Determinação de nitrogênio inorgânico em solo pelo método da destilação a vapor. In *Análise Química para Avaliação da Fertilidade de Solos Tropicais*; Instituto Agronômico: Campinas, Brazil, 2001; p. 285.
32. Thissen, U.; Pepers, M.; Üstün, B.; Melssen, W.J.; Buydens, L.M.C. Comparing support vector machines to PLS for spectral regression applications. *Chemom. Intell. Lab. Syst.* **2004**, *73*, 169–179. [CrossRef]
33. Terra, F.S.; Demattê, J.A.M.; Viscarra Rossel, R.A. Spectral libraries for quantitative analyses of tropical Brazilian soils: Comparing vis–NIR and mid-IR reflectance data. *Geoderma* **2015**, *255–256*, 81–93. [CrossRef]
34. Ribeiro, S.G.; Oliveira, M.R.R.; Lopes, L.M.; Costa, M.C.G.; Toma, R.S.; Araújo, I.C.S.; Moreira, L.C.J.; Teixeira, A.S. Reflectance spectroscopy in the prediction of soil organic carbon associated with humic substances. *Rev. Bras. Cienc. Solo* **2023**, *47*, e0220143. [CrossRef]
35. Yu, P.; Han, K.; Li, Q.; Zhou, D. Soil organic carbon fractions are affected by different land uses in an agro-pastoral transitional zone in Northeastern China. *Ecol. Indic.* **2017**, *73*, 331–337. [CrossRef]
36. Morona, F.; Santos, F.R.; Brinatti, A.M.; Melquiades, F.L. Quick analysis of organic matter in soil by energy-dispersive X-ray fluorescence and multivariate analysis. *Appl. Radiat. Isot.* **2017**, *130*, 13–20. [CrossRef] [PubMed]
37. Blanco-Canqui, H.; Shaver, T.M.; Lindquist, J.L.; Shapiro, C.A.; Elmore, R.W.; Francisco, C.A.; Herget, G.W. Cover crops and ecosystem services: Insights from studies in temperate soils. *Agronomy* **2015**, *107*, 2449–2474. [CrossRef]
38. Branco, C.M.; DuPont, S.T.; Hautau, M.; Hartman, D.; Finney, D.M.; Bradley, B.; LaChance, J.C.; Kaye, J.P. Managing the trade off between nitrogen supply and retention with cover crop mixtures. *Agric. Ecosyst. Environ.* **2017**, *237*, 121–133. [CrossRef]
39. Jian, J.; Lester, B.J.; Du, X.; Reiter, M.S.; Stewart, R.D. A calculator to quantify cover crop effects on soil health and productivity. *Soil. Tillage Res.* **2020**, *199*, 104575. [CrossRef]
40. Campbell, P.M.M.; Fernandes Filho, E.I.; Francelino, M.R.; Demattê, J.A.M.; Pereira, M.G.; Guimarães, C.C.B.; Pinto, L.A.S.L. Digital soil mapping of soil properties in the "Mar de Morros" environment using spectral data. *Rev. Bras. Ciênc. Solo* **2019**, *42*, e0170413. [CrossRef]
41. Rawal, A.; Hartemink, A.; Zhang, Y.; Wang, Y.; Lankau, R.A.; Ruak, M.D. Visible and near-infrared spectroscopy predicted leaf nitrogen contents of potato varieties under different growth and management conditions. *Precis. Agric.* **2023**, *25*, 751–770. [CrossRef]
42. Ghosh, P.K.; Bandyopadhyay, K.K.; Wanjari, R.H.; Manna, M.C.; Misra, A.K.; Mohanty, M. Legume Effect for Enhancing Productivity Nutrient Use-efficiency in major cropping systems—An indian perspective: A review. *J. Sustain. Agric.* **2007**, *30*, 59–86. [CrossRef]
43. Peoples, M.B.; Ladha, J.K.; Herridge, D.F. Enhancing legume N2 fixation through plant and soil management. In *Management of Biological Nitrogen Fixation for the Development of More Productive and Sustainable Agricultural Systems*; Springer: Dordrecht, The Netherlands, 1995; pp. 83–101.

44. Chen, Z.; Ren, S.; Qin, R.; Nile, P. Rapid detection of different types of soil nitrogen using near-infrared hyperspectral imaging. *Molecules* **2022**, *27*, 2017. [CrossRef]
45. Xu, D.; Zhao, R.; Li, S.; Chen, S.; Jiang, Q.; Zhou, L.; Shi, Z. Multi-sensor fusion for the determination of several soil properties in the Yangtze River Delta, China. *Eur. J. Soil. Sci.* **2019**, *70*, 162–173. [CrossRef]
46. Sharma, A.; Weindorf, D.C.; Wang, D.; Chakraborty, S. Characterizing soils via portable X-ray fluorescence spectrometer: 4. Cation exchange capacity (CEC). *Geoderma* **2015**, *239–240*, 130–134. [CrossRef]
47. Zhang, Y.; Hartemink, A.E. Data fusion of vis-NIR and PXRF spectra to predict soil physical and chemical properties. *Eur. J. Soil. Sci.* **2020**, *71*, 316–333. [CrossRef]
48. Greenberg, I.; Vohland, M.; Seidel, M.; Hutengs, C.; Bezard, R.; Ludwig, B. Evaluation of Mid-Infrared and X-ray Fluorescence data fusion approaches for prediction of soil properties at the field scale. *Sensors* **2023**, *23*, 662. [CrossRef] [PubMed]
49. Declercq, Y.; Delbecque, N.; Grave, J.; Smedt, P.; Finke, P.; Mouazen, A.M.; Nawar, D.; Vandenberghe, D.; Meirvenne, M.V.; Verdoodt, A. A comprehensive study of three different portable xrf scanners to assess the soil geochemistry of an extensive sample dataset. *Remote Sens.* **2019**, *11*, 2490. [CrossRef]
50. Ehsani, M.; Upadhyaya, S.K.; Slaughter, D.; Shafii, S.; Pelletier, M. A NIR technique for rapid determination of soil mineral nitrogen. *Precis. Agric.* **1999**, *1*, 219–236. [CrossRef]
51. Espinoza, S.; Ovalle, C.; Del Pozo, A. The contribution of nitrogen fixed by annual legume pastures to the productivity of wheat in two contrasting Mediterranean environments in central Chile. *Field Crops Res.* **2020**, *249*, 107709. [CrossRef]
52. Machado, W.; Franchini, J.C.; Guimarães, M.F.; Filho, J.T. Spectroscopic characterization of humic and fulvic acids in soil aggregates, Brazil. *Heliyon* **2020**, *6*, e04078. [CrossRef]
53. Ghabbour, E.A.; Davies, G.; Sayeed, A.A.; Jenkins, T. Measuring the retained water and sequestered organic carbon contents of soil profiles in aroostook and piscataquis counties, Maine, USA. *Soil. Horiz.* **2013**, *54*, 1–7. [CrossRef]
54. Loss, A.; Pereira, M.G.; Mendes Costa, E.; Beutler, S.J.; Piccolo, M.C. Soil fertility, humic fractions and natural abundance of 13C and 15N in soil under different land use in Paraná State, Southern Brazil. *Idesia* **2016**, *34*, 27–38. [CrossRef]
55. Balabin, R.M.; Safieva, R.Z.; Lomakina, E.I. Comparison of linear and nonlinear calibration models based on near infrared (NIR) spectroscopy data for gasoline properties prediction. *Chemom. Intell. Lab. Syst.* **2007**, *88*, 183–188. [CrossRef]
56. Andersen, C.M. Bro RVariable selection in regression—A tutorial. *J. Chemom.* **2010**, *24*, 728–737. [CrossRef]
57. Stagnari, F.; Maggio, A.; Galieni, A.; Pisante, M. Multiple benefits of legumes for agriculture sustainability: An overview. *Chem. Biol. Technol. Agric.* **2017**, *4*, 2. [CrossRef]
58. Vaudour, E.; Cerovic, Z.; Ebengo, D.; Latouche, G. Predicting Key Agronomic Soil Properties with UV-Vis Fluorescence Measurements Combined with Vis-NIR-SWIR Reflectance Spectroscopy: A Farm-Scale Study in a Mediterranean Viticultural Agroecosystem. *Sensors* **2018**, *18*, 1157. [CrossRef] [PubMed]
59. Sauer, M.; Hofkens, J.; Enderlein, J. *Handbook of Fluorescence Spectroscopy and Imaging: From Ensemble to Single Molecules*, 2011th ed.; John Wiley & Sons, Ltd.: Weinheim, Germany, 2010.
60. Xu, S.; Wang, M.; Shi, X.; Yu, Q.; Zhonggi, Z. Integrating hyperspectral imaging with machine learning techniques for the high-resolution mapping of soil nitrogen fractions in soil profiles. *Sci. Total Environ.* **2021**, *754*, 142135. [CrossRef] [PubMed]
61. Wold, S.; Martens, H.; Wold, H. The multivariate calibration problem in chemistry solved by the PLS method. In *Matrix Pencils. Lecture Notes in Mathematics*; Springer: Berlin/Heidelberg, Germany, 1983; pp. 286–293.
62. Peng, X.; Shi, T.; Song, A.; Chen, Y.; Gao, W. Estimating soil organic carbon using VIS/NIR spectroscopy with SVMR and SPA methods. *Remote Sens.* **2014**, *6*, 2699–2717. [CrossRef]
63. Ge, Y.; Morgan, C.L.S.; Grunwald, S.; Brown, D.J.; Sarkhot, D.V. Comparison of soil reflectance spectra and calibration models obtained using multiple spectrometers. *Geoderma* **2011**, *161*, 202–211. [CrossRef]
64. Zhu, D.; Ji, B.; Meng, C.; Shi, B.; Tua, Z.; Qing, Z. The performance of ν-support vector regression on determination of soluble solids content of apple by acousto-optic tunable filter near-infrared spectroscopy. *Anal. Chim. Acta* **2007**, *598*, 227–234. [CrossRef] [PubMed]
65. Walczak, B.; Massart, D.L. The Radial Basis Functions—Partial Least Squares approach as a flexible non-linear regression technique. *Anal. Chim. Acta* **1996**, *331*, 177–185. [CrossRef]
66. Vasques, G.M.; Grunwald, S.; Sickman, J.O. Modeling of Soil Organic Carbon Fractions Using Visible–Near-Infrared Spectroscopy. *Soil. Sci. Soc. Am. J.* **2009**, *73*, 176–184. [CrossRef]
67. Andrade, R.; Silva, S.H.G.; Weindorf, D.C.; Charkraborty, S.; Faria, W.M.; Mesquita, L.F.; Guilherme, L.R.G.; Curi, N. Assessing models for prediction of some soil chemical properties from portable X-ray fluorescence (pXRF) spectrometry data in Brazilian Coastal Plains. *Geoderma* **2020**, *357*, 113957. [CrossRef]
68. Kirschke, T.; Spott, O.; Vetterlein, D. Impact of urease and nitrification inhibitor on NH_4^+ and NO_3^- dynamic in soil after urea spring application under field conditions evaluated by soil extraction and soil solutions. *J. Plant Nutr. Soil. Sci.* **2019**, *182*, 441–450. [CrossRef]
69. Tomás, F.; Petzold, R.; Solveig, M.; Mollenhauer, H.; Becker, C. Werban, U. Estimating Forest Soil Properties for Humus Assessment—Is Vis-NIR the Way to Go? *Remote Sens.* **2022**, *14*, 1368. [CrossRef]
70. Mohamed, E.S.; El Baroudy, A.A.; El-beshbeshy, T.; Emam, M.; Belal, A.A.; Elfadaly, A.; Aldosari, A.A.; Ali, A.M.; Lasaponara, R. Vis-NIR Spectroscopy and Satellite Landsat-8 OLI Data to Map Soil Nutrients in Arid Conditions: A Case Study of the Northwest Coast of Egypt. *Remote Sens.* **2020**, *12*, 3716. [CrossRef]

71. Ruma, F.Y.; Munnaf, M.A.; Neve, S. Visible and near infrared spectroscopy for predicting soil nitrogen mineralization rate: Effect of incubation period and ancillary soil properties. *Catena* **2024**, *235*, 107649. [CrossRef]
72. Beaudoin, N.; Saad, J.K.; Van Laethem, C.; Machet, J.M.; Maucorps, J.; Maria, B. Nitrate leaching in intensive agriculture in Northern France: Effect of farming practices, soils and crop rotations. *Agric. Ecosyst. Environ.* **2005**, *111*, 292–310. [CrossRef]
73. Asgari, N.; Ayoubi, S.; Demattê, J.A.M.; Dotto, A.C. Carbonates and organic matter in soils characterized by reflected energy from 350–25,000 nm wavelength. *J. Mt. Sci.* **2020**, *17*, 1636–1651. [CrossRef]
74. Linsler, D.; Sawallisch, A.; Höper, H.; Schmidt, H.; Vohland, M.; Ludwig, B. Near-infrared spectroscopy for determination of soil organic C, microbial biomass C and C and N fractions in a heterogeneous sample of German arable surface soils. *Arch. Agron. Soil. Sci.* **2017**, *63*, 1499–1509. [CrossRef]
75. Dalal, R.C. Soil microbial biomass—What do the numbers really mean? *Aust. J. Exp. Agric.* **1998**, *38*, 649. [CrossRef]
76. Nguyen, H.V.-M.; Lee, H.-S.; Lee, S.-Y.; Hur, J.; Shin, H.S. Changes in structural characteristics of humic and fulvic acids under chlorination and their association with trihalomethanes and haloacetic acids formation. *Sci. Total Environ.* **2021**, *790*, 148142. [CrossRef]
77. Franzluebbers, A.J.; Stuedemann, J.A.; Franklin, D.H. Water infiltration and surface-soil structural properties as influenced by animal traffic in the Southern Piedmont USA. *Rev. Agric. Food Syst.* **2012**, *27*, 256–265. [CrossRef]
78. Baldotto, M.A.; Vieira, E.M.; Souza, D.O.; Baldotto, L.E.B. Estoque e frações de carbono orgânico e fertilidade de solo sob floresta, agricultura e pecuária. *Rev. Ceres* **2015**, *62*, 301–309. [CrossRef]
79. Mokany, K.; Raison, R.J.; Prokushkin, A.S. Critical analysis of root: Shoot ratios in terrestrial biomes. *Glob. Chang. Biol.* **2006**, *12*, 84–96. [CrossRef]
80. Santos, N.Z.; Dieckow, J.; Bayer, C.; Molin, R.; Favaretto, N.; Pauletti, V.; Piva, J.T. Forages, cover crops and related shoot and root additions in no-till rotations to C sequestration in a subtropical Ferralsol. *Soil. Tillage Res.* **2011**, *111*, 208–218. [CrossRef]
81. Hu, Y.-L.; Zeng, D.-H.; Ma, X.-Q.; Chang, S.X. Root rather than leaf litter input drives soil carbon sequestration after afforestation on a marginal cropland. *For. Ecol. Manag.* **2016**, *362*, 38–45. [CrossRef]
82. Alyokhin, A.; Nault, B.; Brown, B. Soil conservation practices for insect pest management in highly disturbed agroecosystems—A review. *Entomol. Exp. Appl.* **2020**, *168*, 7–27. [CrossRef]